• Clinical Research •

Biomechanical analysis of an absorbable material for treating fractures of the inferior orbital wall

Jin-Hai Yu[1,2,3,4], *Ze-Xi Sang*[1,2,3,4], *Huang Zhang*[4,5,6], *Qi-Hua Xu*[4,5,6], *Qin Huang*[4,5,6], *Hong-Fei Liao*[4,5,6], *Yao-Hua Wang*[4,5,6]

[1]School of Optometry, Jiangxi Medical College, Nanchang University, Nanchang 330006, Jiangxi Province, China
[2]Jiangxi Research Institute of Ophthalmology and Visual Science, Nanchang 330006, Jiangxi Province, China
[3]Jiangxi Provincial Key Laboratory for Ophthalmology, Nanchang 330006, Jiangxi Province, China
[4]National Clinical Research Center for Ocular Diseases Jiangxi Province Division, Nanchang 330006, Jiangxi Province, China
[5]The Affiliated Eye Hospital, Jiangxi Medical College, Nanchang 330006, Jiangxi Province, China
[6]Jiangxi Clinical Research Center for Ophthalmic Disease, Nanchang 330006, Jiangxi Province, China
Co-first authors: Jin-Hai Yu and Ze-Xi Sang
Correspondence to: Hong-Fei Liao and Yao-Hua Wang. No.463 Bayi Avenue, Nanchang 330006, Jiangxi Province, China. feifei671919@163.com; eye0916@163.com
Received: 2023-08-07 Accepted: 2024-03-29

Abstract

● **AIM:** To investigate the biomechanical properties and practical application of absorbable materials in orbital fracture repair.

● **METHODS:** The three-dimensional (3D) model of orbital blowout fractures was reconstructed using Mimics21.0 software. The repair guide plate model for inferior orbital wall fracture was designed using 3-matic13.0 and Geomagic wrap 21.0 software. The finite element model of orbital blowout fracture and absorbable repair plate was established using 3-matic13.0 and ANSYS Workbench 21.0 software. The mechanical response of absorbable plates, with thicknesses of 0.6 and 1.2 mm, was modeled after their placement in the orbit. Two patients with inferior orbital wall fractures volunteered to receive single-layer and double-layer absorbable plates combined with 3D printing technology to facilitate surgical treatment of orbital wall fractures.

● **RESULTS:** The finite element models of orbital blowout fracture and absorbable plate were successfully established. Finite element analysis (FEA) showed that when the Young's modulus of the absorbable plate decreases to 3.15 MPa, the repair material with a thickness of 0.6 mm was influenced by the gravitational forces of the orbital contents, resulting in a maximum total deformation of approximately 3.3 mm. Conversely, when the absorbable plate was 1.2 mm thick, the overall maximum total deformation was around 0.4 mm. The half-year follow-up results of the clinical cases confirmed that the absorbable plate with a thickness of 1.2 mm had smaller maximum total deformation and better clinical efficacy.

● **CONCLUSION:** The biomechanical analysis observations in this study are largely consistent with the clinical situation. The use of double-layer absorbable plates in conjunction with 3D printing technology is recommended to support surgical treatment of infraorbital wall blowout fractures.

● **KEYWORDS:** orbital blowout fracture; absorbable material; finite element analysis; 3D printing technology
DOI:10.18240/ijo.2024.07.19

Citation: Yu JH, Sang ZX, Zhang H, Xu QH, Huang Q, Liao HF, Wang YH. Biomechanical analysis of an absorbable material for treating fractures of the inferior orbital wall. *Int J Ophthalmol* 2024;17(7):1331-1336

INTRODUCTION

Orbital blowout fractures can result in symptoms such as enophthalmos, diplopia, eye movement disorders, and numbness in the infraorbital region, significantly impacting the visual function and aesthetic appearance of patients[1]. If these symptoms do not improve with conservative treatment, surgery becomes the primary approach for intervention. Several factors influence the therapeutic outcomes of orbital fracture surgery, including the timing of surgery, surgical approach, choice of repair materials, and the surgeon's experience. In recent years, advancements in three-dimensional (3D) printing technology have led to increased precision and personalization in orbital fracture repair surgery[2]. With the aid of digital medical imaging technology, researchers can utilize the 3D morphology of the patient's unaffected orbit to simulate and reconstruct the 3D structure of the injured orbital bone wall following repair. A

surgical guide for precise shaping of the repair material can be designed based on the 3D structural model of the reconstructed orbit. The anatomical repair of the fractured defect area can be achieved during the surgery using the assistance of the 3D-printed orbital model and surgical guide[3].

Orbital fracture surgery assisted by 3D printing technology can enhance surgical success rates and decrease complication rates. However, it is ineffective against associated complications, such as implant rejection or infection resulting from the restorative material[4]. Common orbital fracture repair materials include hydroxyapatite bone plates, high-density porous polyethylene (Medpor), titanium mesh, Medpor titanium mesh (Medpor-Titan), and absorbable materials. Absorbable materials are primarily utilized for repairing orbital blowout fractures in children due to their ability to degrade and be absorbed in the body, resulting in fewer complications related to implant materials compared to other repair materials. Absorbable materials are also a viable choice for orbital blowout fractures in adults. The key concern is whether the absorbable material can offer sufficient support for repairing the defect in the orbital wall[5].

Recently, researchers have investigated the mechanism of orbital fractures using finite element biomechanical analysis techniques and validated their findings through experimental studies[6]. Owing to its exceptional simulation capabilities, this technology has been utilized and analyzed in investigating mechanical issues across various areas of orbital diseases. Nevertheless, there is limited research on the biomechanical analysis of absorbable materials in orbital blowout fractures. This study aims to employ finite element biomechanical analysis technology to investigate the mechanical impact of absorbable materials in the repair of orbital wall defects, thereby offering valuable insights for clinical practice.

SUBJECTS AND METHODS

Ethical Approval The study complied with the Helsinki Declaration and was approved by the Medical Ethics Committee of the Affiliated Eye Hospital of Nanchang University (Protocol No.YLP20220501). All patients signed the informed consent form for the study.

Equipment and Software The equipment and software used in this study included a 64-slice spiral computed tomography (CT) machine (SIEMENS, Germany), LAPTOP-BHLLMTH1 (Lenovo, China), Form2 printer (KONICA MINOLTA, Japan), absorbable plate poly-L/DL-lactide trimethylene carbonate (PLT; Inion Oy, Finland), Mimics21.0 software (Materialise Company, Belgium), 3-matic13.0 software (Materialise Company, Belgium), Geomagic wrap 21.0 (Geomagic Company, USA), and ANSYS Workbench 21.0 software (ANSYS Company, USA).

Establishment of 3D Models A volunteer with orbital blowout fracture in the left eye resulting from a boxing injury underwent orbital CT scan with a slice thickness of 0.6 mm. The acquired medical digital image and communication (Digital Imaging and Communications in Medicine, DICOM) file data were burned to a compact disc. The Mimics21.0 software was used to select the threshold range for bone as a mask, allowing segmentation of the imported DICOM data from the compact disc on a laptop. Manual delineation of the normal bony structure of the inferior and inner orbital walls was performed. The mask data was processed to generate a 3D model of the orbital fracture, which was saved in the stereolithography (STL) file format. The STL data was imported into 3-matic13.0 software, and the model underwent wrapping, reduction, and smoothing optimization operations. Furthermore, the three-point method was employed to establish a sagittal center plane. The model was mirrored based on this plane to create a mirrored model. A Boolean union operation was performed on the two models to create a new model, which was then saved in STL format. The newly generated STL data file was imported into the reverse engineering software Geomagic wrap 21.0. The “curve cutting” command was utilized to create a curved surface along the edge of the fracture area, and the “shell” command was employed to generate a guide plate for repairing the bone wall defect. The resulting guide plate was saved in STL format. To analyze the biomechanics of absorbable plates with two different thicknesses in orbital blowout fractures, two guide plate models with thicknesses of 0.6 and 1.2 mm were created.

Finite Element Model Establishment The STL file of the guide plate was imported into the 3-matic13.0 software. The “2D Linear Pattern” and “2D to 3D Linear Pattern” commands in the texture module were utilized to create a hole texture on the guide plate, similar to the absorbable plate. The 3D model of the orbital fracture and the guide plate were meshed to generate a tetrahedral 10-node unit solid model, which was then saved in CDB format. The CDB file was imported into the static structure analysis module of ANSYS Workbench 21.0 software through the external module. Bone tissue and absorbable material were assumed to be isotropic, homogeneous, linear elastic materials. The material properties of the orbital bone and absorbable plates were assigned based on literature reports[7].

Boundary Condition Setting The contact relationship between the absorbable plate and the edge of the defect area was set as bonded. The suborbital axial section was set as a fixed plane. To simulate the support force of the absorbable plate on the orbital content, a 0.3N load in the direction of gravity was applied to the absorbable plate. The contact surface between the absorbable plate and the orbital content served as the acting surface. The extent and scope of Young’s modulus reduction in absorbable materials during the degradation

Table 1 Results of finite element analysis for absorbable plates with different thicknesses under various simulated Young's modulus decay conditions

Young's modulus (MPa)	Absorbable plate with a thickness of 0.6 mm			Absorbable plate with a thickness of 1.2 mm		
	Total deformation	Equivalent stress	Equivalent strain	Total deformation	Equivalent stress	Equivalent strain
3150	3.3988e-3	0.89414	3.5626e-4	4.64e-4	0.21668	7.6095e-5
315	3.3607e-2	0.89514	3.546e-3	4.4458e-3	0.21264	7.5157e-4
31.5	0.33567	0.8952	3.5441e-2	4.4251e-2	0.21213	7.503e-3
3.15	3.3563	0.89521	0.35439	0.4423	0.21207	7.5016e-2

process are elucidated based on relevant research reports[8-9], In this study, the 10-fold gradient decay of the Young's modulus of the material was simulated after shaping the absorbable plate, considering the degradation and absorption process in the implanted body. The equivalent Von-Mises stress, equivalent elastic strain, and peak total deformation of the material were computed under the same boundary conditions for one-layer and two-layer absorbable plates.

Clinical Case Verification Two patients with orbital blowout fractures, who underwent orbital fracture repair surgery with the assistance of absorbable materials combined with 3D printing technology, were recruited as volunteers. The orbital and guide models of the two patients were printed using a Form2 printer. During the operation, one-layer and two-layer absorbable plates were used, and the imaging data and clinical outcomes were assessed at one week and six months post-operation. To assess the clinical significance of biomechanical analysis of absorbable materials in orbital blowout fractures

RESULTS

3D Model The orbital CT data of the volunteers were processed using Mimics21.0 software, 3-matic13.0 software, and Geomagic wrap 21.0 software to generate the 3D model of the orbital blowout fracture and the repair guide plate model (Figure 1).

Finite Element Model The finite element solid models for repairing orbital blowout fractures with one-layer and two-layer absorbable plates were obtained using 3-matic13.0 software and ANSYS Workbench 21.0 software. The absorbable sheet had a layer thickness of 0.6 mm and a porous structure, which matched the specifications of the actual absorbable sheet PLT (Inion Oy, Finland). The finite element model of the one-layer absorbable plate comprised 66 715 nodes and 33 754 elements, while the finite element model of the orbital fracture comprised 89 580 nodes and 48 705 elements (Figure 2).

Results of Finite Element Analysis The Young's modulus of absorbable materials continues to decay until it completely disappears during the process of degradation and absorption in the body. The equivalent stress of the 0.6 mm thick absorbable plate is approximately 4.2 times higher than that of the 1.2 mm thick absorbable plate, and the stress value remains unaffected by changes in Young's modulus. The equivalent strain of the 0.6 mm thick absorbable plate is approximately 4.6 times higher than that of the 1.2 mm thick absorbable plate, and the strain value increases as the Young's modulus decreases. The total deformation of the 0.6 mm thick absorbable plate is approximately 7.6 times higher than that of the 1.2 mm thick absorbable plate. At a Young's modulus decay of 3.15 MPa, the maximum deformation of the 0.6 mm thick absorbable plate is approximately 3.3 mm (Table 1, Figure 3).

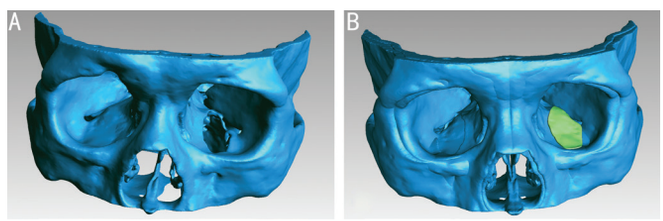

Figure 1 Three-dimensional models of orbital blowout fracture and repair guide plate A: The orbital blowout fracture model; B: The fracture model and the repair guide plate model after mirror image merging.

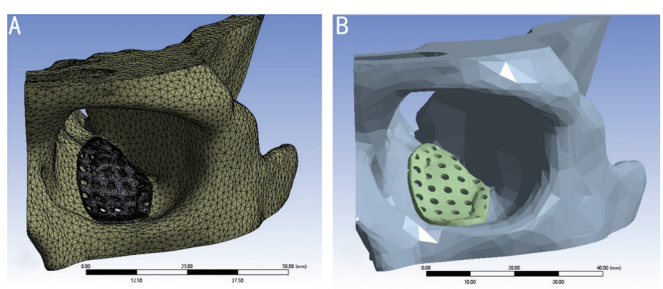

Figure 2 Finite element models of orbital blowout fracture repaired with absorbable plates A: The meshed finite element model of the eye orbit repaired using a single layer of absorbable plate; B: The finite element model of the eye orbit repaired with two layers of absorbable plate.

Table 1 shows the maximum total deformation, maximum equivalent stress, and maximum equivalent strain of absorbable plates with two thicknesses under various Young's modulus attenuation simulations under the influence of orbital content gravity.

Results of Clinical Case Study Both volunteer A and volunteer B experienced left inferior orbital wall fractures resulting from boxing injuries, and the sizes of the orbital wall defects were approximately equal. Both volunteers underwent orbital fracture repair surgery with the assistance of absorbable materials and 3D printing technology. Both volunteers experienced diplopia and eye movement disturbances prior

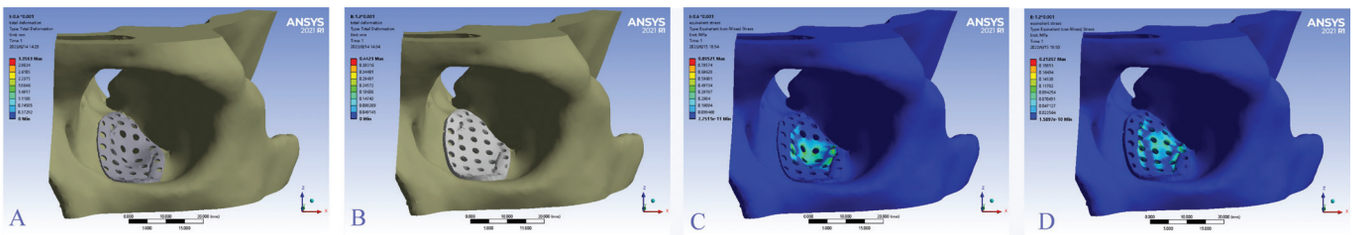

Figure 3 The maximum total deformation (A, B) and equivalent stress (C, D) of the absorbable plate with a thickness of 0.6 (A, C) and 1.2 mm (B, D), respectively, when the Young's modulus decays to 3.15 MPa under the influence of orbital content gravity.

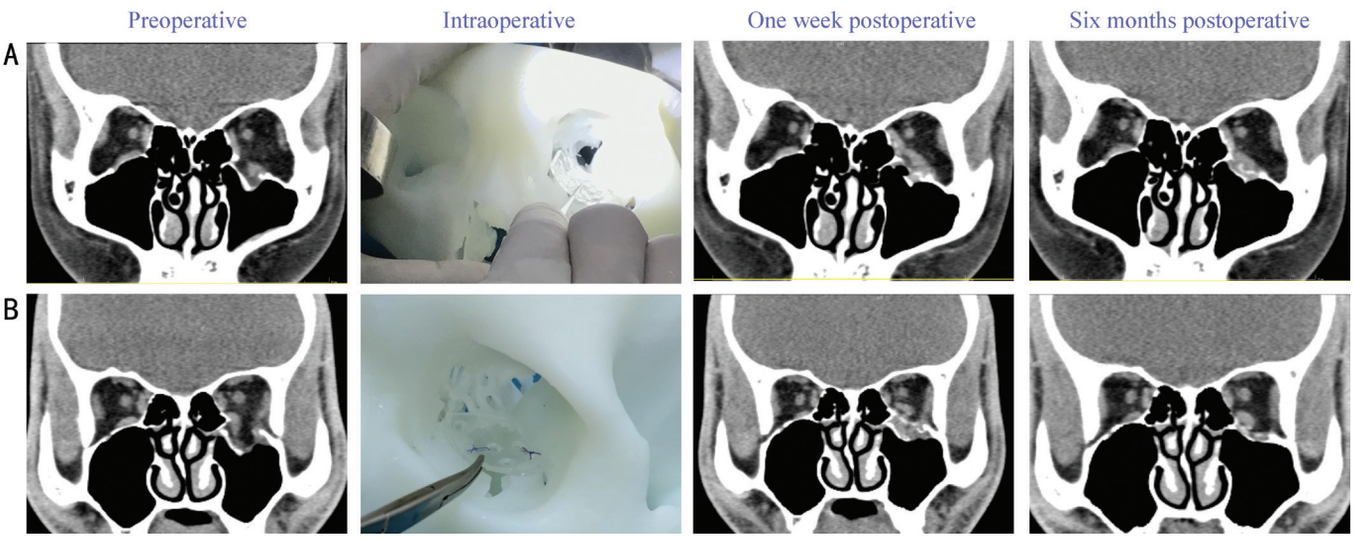

Figure 4 Coronal CT images of volunteers A and B before the surgery, 1wk, and 6mo after the surgery It also shows the utilization of absorbable materials combined with 3D printing models to aid in orbital fracture repair during the operation. CT: Computed tomography.

to the surgery. Volunteer A had exophthalmos measurements of oculus dexter (OD): 14 mm, outer canthal distance (OCD): 100 mm, oculus sinister (OS): 11 mm. Volunteer B had exophthalmos measurements of OD: 13 mm, OCD: 98 mm, OS: 10 mm. Volunteer A received a single-layer absorbable plate (Inion Oy, Finland) with a thickness of 0.6 mm during the surgery, while Volunteer B received two layers of absorbable plates (Inion Oy, Finland) with a thickness of 0.6 mm. Coronal CT scans conducted 1wk after the surgery confirmed the proper anatomical positioning of the absorbable plate repair materials in both volunteers. Both volunteers experienced a return to normal vision and oculomotor function following the surgery. Six months after the surgery, the coronal CT scan revealed a concave and deformed shape of the absorbable plate in volunteer A, whereas the shape of the absorbable plate in volunteer B remained unchanged. Volunteer A had exophthalmos measurements of OD: 14 mm, OCD: 100 mm, OS: 12 mm. Volunteer B had exophthalmos measurements of OD: 13 mm, OCD: 98 mm, OS: 13 mm (Figure 4).

DISCUSSION

Currently, absorbable polymers primarily consist of polylactic acid (PLLA), polyglycolic acid (PGA), poly-L/DL-lactide (PLDL), poly-L-lactic acid-trimethylene carbonate (PLTMC), and polycaprolactone (PCL), among others. The majority of absorbable materials are produced by blending two polymers in specific proportions. Various absorbable materials degrade at distinct rates within the body, which are influenced by factors including the molecular weight of the material, the ratio of components in the formulation, crystallinity, as well as environmental conditions such as temperature and humidity. The absorbable plate used in this study, PLT (Inion Oy, Finland), was fabricated by combining PLDL and PLTMC. Several studies have indicated a significant decrease in the initial Young's modulus of absorbable materials after shaping[10]. Therefore, some scholars have proposed that the analysis of absorbable materials should focus more on the therapeutic force rather than the initial force[11]. The mechanical properties of absorbable materials decline during the degradation process. Higher probability of postoperative enophthalmos complications is associated with material degradation rates surpassing the bone healing rate in the bone wall defect area[12].

Finite element analysis (FEA) in this study reveals that as the Young's modulus of the absorbable plate decays to 3.15 MPa the 0.6 mm thick repair material undergoes a maximum deformation of approximately 3.3 mm due to the gravitational force of the orbital content. Conversely, a 1.2 mm thick absorbable plate exhibits an overall maximum deformation

of around 0.4 mm. These findings suggest that the use of two-layer absorbable plates for repairing inferior wall orbital blowout fractures minimizes the mechanical instability of the absorbable material. However, although clinical cases indicated no changes in the form of the absorbable material 1wk post-surgery, imaging data taken half a year later revealed concave deformation in the 0.6 mm thick absorbable plate. This deformation indirectly resulted in slight enophthalmos of volunteer A's left eye 6mo after the operation. Volunteer B, who received a 1.2 mm thick absorbable plate implant, did not exhibit changes in the shape of the repair material or enophthalmos. The findings of the FEA aligned closely with the imaging data obtained half a year post-surgery in clinical cases. It is possible that during the early stage, absorbable plates with different thicknesses exhibited some variations in shape change. However, due to the short duration of the study, these shape changes were not significant. Over time, the degradation of absorbable materials leads to a reduction in Young's modulus[13]. Prolonged action over a period of 6mo leads to visible concave deformation, resulting from the cumulative effects of absorbable plate's shape change, degradation, and material absorption. These findings suggest that biomechanical analysis of absorbable materials in orbital blowout fractures can to some extent simulate the mechanical conditions of repair materials more realistically. Based on clinical case results, we believe that combining absorbable materials with 3D printing technology in orbital blowout fractures can achieve anatomical repair of orbital wall defects. Implanting and repairing thick absorbable plates is an effective method to prevent long-term complications of enophthalmos following surgery.

FEA is commonly utilized in the study of orbital diseases, particularly in investigating the mechanisms of orbital fractures, traumatic optic nerve injury, and analyzing the force exerted by extraocular muscles in thyroid associated ophthalmopathy[14-16]. A biomechanical analysis was conducted by some scholars to investigate the reoccurrence of orbital injury after implanting a titanium mesh in orbital fractures. The findings suggest that the titanium mesh may potentially cause trauma to the orbital tissue[17]. This also indirectly suggests that the utilization of absorbable materials may reduce the risk of orbital tissue trauma. Early scholars have analyzed the biomechanics of absorbable materials in orbital fractures[18]. Nevertheless, the mesh division in the finite element model of the absorbable plate is relatively coarse, and the overall model structure is relatively simplistic. Additionally, the research did not incorporate the verification of clinical cases, which significantly impacted the credibility of the research findings. Biomechanical analysis in ophthalmology encompasses measuring corneal elastic characteristics in glaucoma[19], evaluating the impact of orthokeratology on myopic patients' corneal morphology[20], and assessing changes posterior corneal surface elevation post-corneal laser surgery[21]. Instruments used for these measurements yield stable data with good repeatability. However, the accuracy of biomechanical analysis results using finite element methods may be influenced by various factors. Researchers have demonstrated the feasibility of using FEA models for assessing orbital development biomechanics with clinical data from congenital microphthalmia patients[22], indirectly supporting the accuracy of our research.

However, our study shares the limitations commonly observed in finite element biomechanical analyses. In reality, the orbital bone tissue and the absorbable plate are anisotropic nonlinear elastic materials, contrary to the assumption made in this study of them being isotropic linear elastic materials. Our simulation employs overly idealized boundary conditions and relatively simplistic contact relationships, deviating from the complexities of the actual scenario. Conversely, the establishment of the orbital finite element model currently lacks a unified method, leading researchers to employ diverse software and modeling techniques, potentially yielding inconsistent outcomes[23]. Finite element biomechanical analysis aids doctors in simulating stress and strain conditions in various clinical case scenarios, offering valuable reference and guidance for clinical treatment plans. Nevertheless, the outcomes of FEA cannot be directly translated into clinical practice due to their approximation to real-world conditions. The reliability of the results must be confirmed through real-world tests or clinical cases to establish their reference value. Importantly, in this study, we observed through clinical case verification that the implantation of a 2-layer thick absorbable plate can maintain favorable mechanical support even after six months. By integrating the findings from FEA and the validation of clinical cases, we assert that finite element biomechanical analysis can provide a more realistic simulation of the mechanical behavior and scenarios involving absorbable plates in orbital blowout fractures. Therefore, we recommend utilizing 3D printing technology in combination with absorbable plates of varying thicknesses for the repair of infraorbital wall fractures.

In conclusion, based on comprehensive FEA and clinical validation, we have determined that utilizing a two-layer absorbable plate could serve as an effective approach for addressing infraorbital wall blowout fractures. This approach aims to mitigate mechanical instability inherent in absorbable materials and offer enduring mechanical support for fracture site healing. Conversely, employing a single-layer absorbable plate of thickness may predispose patients to postoperative complications such as enophthalmos. Therefore, integrating 3D

printing technology with absorbable plates of suitable thickness holds promise for achieving precise anatomical reconstruction of orbital wall defects and diminishing postoperative complications. Although FEA furnishes valuable insights into simulating the mechanical behavior of absorbable materials in orbital fracture repair, its applicability in real-world scenarios necessitates validation through clinical practice. Thus we advocate for judicious selection of absorbable plates, particularly two-layer configurations, in the management of infraorbital wall blowout fractures, supplemented by advanced 3D techniques, to enhance patient outcomes and diminish postoperative complications.

ACKNOWLEDGEMENTS

Foundations: Supported by the National Natural Science Foundation of China (No.82060181); General Project funded by the Jiangxi Provincial Department of Education (No. GJJ2200194).

Conflicts of Interest: Yu JH, None; **Sang ZX,** None; **Zhang H,** None; **Xu QH,** None; **Huang Q,** None; **Liao HF,** None; **Wang YH,** None.

REFERENCES

1 Rajantie H, Kaukola L, Snäll J, Roine R, Sintonen H, Thorén H. Health-related quality of life in patients surgically treated for orbital blow-out fracture: a prospective study. *Oral Maxillofac Surg* 2021;25(3):373-382.

2 Ma CY, Wang TH, Yu WC, *et al*. Accuracy of the application of 3-dimensional printing models in orbital blowout fractures-a preliminary study. *Ann Plast Surg* 2022;88(1s Suppl 1):S33-S38.

3 Liao HF, Yu JH, Hu CQ, Hu XY, Liu Q, Wang YH, Wang AA, Xu QH. Application of three-dimensional printing combined with surgical navigation and endoscopy in orbital fracture reconstruction. *Zhonghua Yan Ke Za Zhi* 2019;55(9):658-664.

4 Ramji HF, Blessing NW, Tan JF, Moreau A. Do orbital implants differ in complication rates: a retrospective study of 88 patients, and an argument for cost-effective practices in the face of rising health care costs. *Facial Plast Surg* 2022;38(3):293-299.

5 Yu JH, Xu QH, Wang YH, Liao HF. Advances in the research and application of orbital blowout fracture repair material. *Zhonghua Yan Ke Za Zhi* 2019;55(11):876-880.

6 Darwich A, Attieh A, Khalil A, Szávai S, Nazha H. Biomechanical assessment of orbital fractures using patient-specific models and clinical matching. *J Stomatol Oral Maxillofac Surg* 2021;122(4):e51-e57.

7 Jung BT, Kim WH, Park B, Lee JH, Kim B, Lee JH. Biomechanical evaluation of unilateral subcondylar fracture of the mandible on the varying materials: a finite element analysis. *PLoS One* 2020;15(10):e0240352.

8 Felfel RM, Poocza L, Gimeno-Fabra M, *et al*. *In vitro* degradation and mechanical properties of PLA-PCL copolymer unit cell scaffolds generated by two-photon polymerization. *Biomed Mater* 2016;11(1):015011.

9 Dumitru AC, Espinosa FM, Garcia R, *et al*. *In situ* nanomechanical characterization of the early stages of swelling and degradation of a biodegradable polymer. *Nanoscale* 2015;7(12):5403-5410.

10 Ballard TN, Kelly KJ, Zaydfudim V, Walcutt NL, Lahijani SS, Shack RB, Thayer WP. Absorbable plate strength loss during molding. *J Craniofac Surg* 2010;21(3):644-647.

11 Bezrouk A, Hosszu T, Hromadko L, *et al*. Mechanical properties of a biodegradable self-expandable polydioxanone monofilament stent: *in vitro* force relaxation and its clinical relevance. *PLoS One* 2020;15(7):e0235842.

12 Esmail MEK, Ibrahiem MFK, Abdallah RMA, Elshafei AMK, Gawdat TI. Resorbable polylactic acid polymer plates in repair of blow-out orbital floor fractures. *Eur J Ophthalmol* 2021;31(3):1384-1390.

13 Dargaville BL, Vaquette C, Peng H, *et al*. Cross-linked poly (trimethylene carbonate-co-L-lactide) as a biodegradable, elastomeric scaffold for vascular engineering applications. *Biomacromolecules* 2011;12(11):3856-3869.

14 Jeong BC, Lee C, Park J, Ryu D. Identification of optimal surgical plan for treatment of extraocular muscle damage in thyroid eye disease patients based on computational biomechanics. *Front Bioeng Biotechnol* 2022;10:969636.

15 Moura LB, Jürgens PC, Gabrielli MAC, Pereira Filho VA. Dynamic three-dimensional finite element analysis of orbital trauma. *Br J Oral Maxillofac Surg* 2021;59(8):905-911.

16 Nagasao T, Morotomi T, Kuriyama M, Tamai M, Sakamoto Y, Takano N. Biomechanical analysis of likelihood of optic canal damage in peri-orbital fracture. *Comput Assist Surg* 2018;23(1):1-7.

17 Foletti JM, Martinez V, Haen P, Godio-Raboutet Y, Guyot L, Thollon L. Finite element analysis of the human orbit. Behavior of titanium mesh for orbital floor reconstruction in case of trauma recurrence. *J Stomatol Oral Maxillofac Surg* 2019;120(2):91-94.

18 Al-Sukhun J, Penttilä H, Ashammakhi N. Orbital stress analysis: part III: biomechanics of orbital blowout fracture repair using bioresorbable poly-L/DL-lactide (PL/DLLA 70:30) implant. *J Craniofac Surg* 2011;22(4):1299-1303.

19 Caride SG, González LP, Francés FS, Feijoo JG. Study of corneal biomechanical properties in patients with childhood glaucoma. *Int J Ophthalmol* 2020;13(12):1922-1927.

20 Nieto-Bona A, Porras-Ángel P, Ayllón-Gordillo AE, Carracedo G, Piñero DP. Short and long term corneal biomechanical analysis after overnight orthokeratology. *Int J Ophthalmol* 2022;15(7):1128-1134.

21 Li ZJ, Yang C, Liu SH, Guo J, Duan YH. Changes in corneal biomechanics and posterior corneal surface elevation after FS-LASIK. *Int J Ophthalmol* 2023;16(11):1832-1837.

22 Song DY, Zhang JW, Yuan BW, Rong QG, Li DM. A finite element analysis model is suitable for biomechanical analysis of orbital development. *J Craniofac Surg* 2021;32(7):2546-2550.

23 Foletti JM, Martinez V, Graillon N, Godio-Raboutet Y, Thollon L, Guyot L. Development and validation of an optimized finite element model of the human orbit. *J Stomatol Oral Maxillofac Surg* 2019;120(1):16-20.